Improved DORT for Breast Cancer Detection in Low Contrast Scenarios

Md. Delwar Hossain and Ananda Sanagavarapu Mohan
Centre for Health Technologies, Faculty of Engineering and IT
University of Technology Sydney
Sydney, Australia
Ananda.Sanagavarapu@uts.edu.au

***Abstract*—Microwave imaging performance deteriorates with increasing clutter and heterogeneity in the imaging medium. Breast cancer detection becomes increasingly challenging with increasing breast density. Decomposition of the time reversal operator (DORT) uses signal subspace of the multistatic matrix which is perturbed in highly heterogeneous medium. To overcome the problem we propose coherent processing in frequency domain prior to imaging operation. Coherent DORT (C-DORT) provides robust imaging performance compared to conventional non-coherent DORT in cluttered medium as evident from the imaging results obtain using anatomically realistic numerical breast phantoms.**

Keywords—breast cancer; coherent focusing; dense breast; DORT; microwave imaging; signal subspace; time reversal;

I. INTRODUCTION

Time reversal microwave imaging is a very useful tool for localizing embedded targets or scatterers in a medium. Time reversal has been introduced initially for acoustics and later on extended for microwaves. Time reversal localization requires multistatic measurement of the object under investigation. The resultant multistatic matrix is used for computational imaging. The imaging process assumes that the background medium is known, lossless and non-dispersive. DORT and time reversal MUSIC (TR-MUSIC) are two widely used subspace based popular time reversal imaging techniques that require orthogonal decomposition of the multistatic matrix or equivalently the time reversal operator (TRO) [1]. DORT uses the signal subspace of the TRO or multistatic matrix is consequently more robust than TR-MUSIC in cluttered medium. When point targets are embedded in a homogeneous background medium, the eigen vectors of the TRO are related in a one-to-one manner with the targets. However, non-point targets can produce multiple eigen values [2] and the presence of strong clutter creates multipath effect resulting in correlated signals in the recorded multistatic matrix. This effect may perturb the multistatic matrix, introducing random phase variations in each frequency bin when processed in frequency domain. Hence, inconclusive results are often obtained when frequency bins of the multistatic matrix are used individually for time reversal imaging.

Time reversal technique has been used in various applications including biomedical imaging for breast cancer screening [3-8] where it exploits the dielectric contrast between tumor and other healthy breast tissues [9, 10]. Breast is a highly heterogeneous mass of different types of glandular and fatty tissues. Glandular tissues have much higher permittivity compared with fatty breast tissues. Breast tissue composition changes with age and various other factors. The malignant lesion is stronger scatterer for incident microwave field than other breast tissues. However, dominant glandular tissue composition of the breast can effectively mask the backscattering from malignant tissue due to diminishing dielectric contrast. As a result it is quite challenging to detect breast cancer in dense breasts [11].

In order to overcome the drawbacks of conventional time reversal DORT imaging technique in a cluttered medium, we propose coherent processing. The TRO will be first obtained over a number of frequency bins using conventional, incoherent approach. Later, using the proposed processing, coherently focused TRO is obtained prior to imaging operation. In a cluttered medium, the signal subspace can become non-uniform when calculated over a wide bandwidth since signals at individual frequency bins may experience random phase variations due to clutter. Coherent processing seeks to transform the individual, in-coherent, frequency bins into a coherently focused bin by minimizing the focusing error [12].

A wavefield modeling based coherent time reversal imaging technique was proposed in [8]. But it may not be suitable with subspace based time reversal techniques due to resultant higher focusing error [13]. Hence, in this paper, we choose coherent signal subspace focusing as our focus is the DORT which is a sub-space based technique. The coherently focused DORT (C-DORT) is obtained by coherently focused TRO which minimizes the effects of random variations experienced in individual frequency bins. Thus, the proposed Coherent-DORT (C-DORT) improves the imaging performance in a dense breast medium. In order to demonstrate its performance, we conduct numerical trials using anatomically realistic numerical 3-D breast phantoms. The results indicate that C-DORT is superior to and more effective than conventional time reversal imaging methods in dense breasts. Our paper is organized as follows. We provide the details of forward problem in section II which will be followed by explanation of proposed C-DORT in section III. The results obtained from numerical phantoms are presented in section IV

and finally the conclusions of the study are provided in section V.

II. Forward Data Conditioning

We use anatomically realistic numerical breast phantoms obtained from UWCEM phantom repository [14] with FDTD simulation to compute the scattered field response from the breast phantom. We consider a cylindrical array of 115 ideal antenna elements to record the scattered field response. The dielectric properties of various breast tissue are computed using single pole Debye parameters [9, 10]. A breast phantom and antenna array element locations are illustrated in Fig. 1. A tumor is artificially introduced into the breast phantom. The breast is illuminated by a differentiated Gaussian pulse of 3-dB bandwidth 1.5-5 GHz and center frequency 3GHz. The FDTD grid size is set to 0.5 mm in all directions. In order to minimize skin reflections, a matching liquid is used to immerse the breast phantom and the antenna array in FDTD simulation. However, matching liquid cannot completely eliminate skin artifacts and further processing for early-time artifact removal is required. Once the skin reflection is removed from the early time response, the scattered field data is further processed for time reversal imaging.

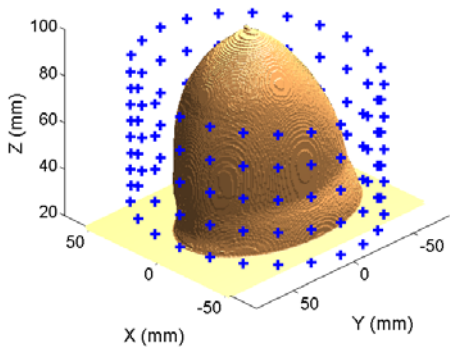

Fig. 1. Breast phantom and antenna array.

A. Skin Artifact Removal

The skin tissue has much higher dielectric constant than the fatty tissues of the breast. As a result the skin tissue highly reflects back the incident microwave field. The tumor can be located deep inside the breast and consequently tumor response in the late time content can be very weak. It is thus very important to remove the early time skin response without affecting the late time response. However, practically breasts are unsymmetrical and the distances between the antenna elements and skin tissue at different locations are different. Considering these practical problems we have developed wavelet and entropy based hybrid skin artifact removal technique. Initially the scattered fields are classified into different groups based on their time of arrivals (TOAs) at different antenna elements using wavelet transform. We use complex continuous wavelet transform (CWT) to estimate TOAs of the received signals. The CWT can be defined as

$$W_s(a,\tau) = s(\tau) * \left(\frac{1}{\sqrt{a}} \psi_n^*(\frac{\tau}{a}) \right) \quad (1)$$

where, $\psi_n(t) = C_n \frac{d^n}{dt^n}(e^{-jt}e^{-t^2})$, C_n is a normalization constant. We carry out CWT of the scattered fields and corresponding excitation signal using $\psi_n(t)$ and estimate TOA from the cross wavelet spectrum. Received signals are then grouped according to their TOAs.

We compute the entropy of each group to obtain entropy based windows. Entropy above a threshold is regarded as skin reflection and can be removed. We consider α-th order Renyi entropy [15] for a group of M antenna elements defined as

$$H_\alpha(t) = \frac{1}{1-\alpha} \log \left\{ \sum_{m=1}^{M} [p_m(t)]^\alpha \right\} \quad (2)$$

where, $p_m(t)$ is the normalized signal at m-th antenna element in the group and α is a real positive constant.

III. Coherent DORT

For coherent DORT (C-DORT) imaging, we need to first obtain the multistatic data matrix from the breast medium. We consider that there are N antenna elements in the array located at $\mathbf{r}_n^t$, where n = 1,2,..N. We also assume that there are P isotropic targets embedded in the background medium whose locations are denoted by $\mathbf{r}_P^o$ where, where p = 1,2,..P. The multistatic matrix in this case can be expressed as

$$\overline{\mathbf{K}} = \overline{\boldsymbol{\mathcal{G}}}\,\overline{\boldsymbol{\chi}}\,\overline{\boldsymbol{\mathcal{G}}}^T \quad (3)$$

where, $\overline{\boldsymbol{\mathcal{G}}}$ is a matrix of background medium Green's function vector, and $\overline{\boldsymbol{\chi}}$ is a matrix representing the scattering strengths of the scatterers. The TRO can now be expressed as

$$\overline{\mathbf{T}}(\omega) = \overline{\mathbf{K}}^H(\omega)\overline{\mathbf{K}}(\omega) \quad (4)$$

A. Coherent Focusing for TRO

The time reversal operator (TRO) given in (4) is non-coherent since the TROs are obtained independently at each frequency bin. In a cluttered medium, the received signals can be highly correlated resulting in correlated frequency bins. As a result sub-space based imaging techniques demonstrate poor performance. We propose to obtain a coherently focused TRO using coherent signal subspace processing. The coherent TRO is obtained by minimizing the focusing error as shown below

$$\min_{\overline{\mathbf{Z}}(\omega_f)} E_{\mathbf{r}^o} \left\{ \left\| \overline{\mathbf{K}}(\omega_o) - \overline{\mathbf{Z}}(\omega_f)\overline{\mathbf{K}}(\omega_f) \right\|_F^2 \right\} \quad \textit{subject to } \overline{\mathbf{Z}}\overline{\mathbf{Z}}^H = \overline{\mathbf{I}} \quad (5)$$

where, $\|.\|_F$ denotes Frobenius norm and $E\{.\}$ denotes expectation. The solution for focusing matrix can be obtained as $\overline{\mathbf{Z}} = \overline{\mathbf{V}}\overline{\mathbf{U}}^H$ where $\overline{\mathbf{K}}^H(\omega_f)\overline{\mathbf{K}}(\omega_o) = \overline{\mathbf{U}}\overline{\boldsymbol{\Sigma}}\overline{\mathbf{V}}^H$ and ω_f ,(f

=1,2,…,*F)* frequency bins are coherently focused into ω_o. We can obtain C-TRO as

$$\overline{\mathbf{T}}_C(\omega_o) = \sum_{f=1}^{F} \overline{\mathbf{Z}}(\omega_f)\overline{\mathbf{T}}(\omega_f)\overline{\mathbf{Z}}^H(\omega_f) \tag{6}$$

Thus, instead of imaging at each frequency bin, C-TRO can be used for coherent time reversal imaging. This also saves computational time, since imaging operation is carried out only for C-TRO.

B. Imaging Function

The vector space of C-TRO, $\overline{\mathbf{T}}_C$ can be expressed in terms of its signal and noise subspaces as follows.

$$\overline{\mathbf{T}}_C = \overline{\mathbf{V}}_{\mathbb{S}}^C \overline{\mathbf{\Sigma}}_{\mathbb{S}}^{C^2} \overline{\mathbf{V}}_{\mathbb{S}}^{C^H} + \overline{\mathbf{V}}_{\mathbb{N}}^C \overline{\mathbf{\Sigma}}_{\mathbb{N}}^{C^2} \overline{\mathbf{V}}_{\mathbb{N}}^{C^H} \tag{7}$$

Since, we are using unitary focusing matrix, the two orthogonal subspaces remain orthogonal in the focused frequency bin. The signal subspace of $\overline{\mathbf{T}}_C$ is spanned by the eigen vectors contained by $\overline{\mathbf{V}}_{\mathbb{S}}^C$ corresponding to the significant eigen values in $\overline{\mathbf{\Sigma}}_{\mathbb{S}}^{C^2}$. The green's function vector forms the orthonormal bases for the eigen vectors. Hence, the C-DORT imaging function is obtained as

$$I_{C-DORT}(\mathbf{r}) = \sum_{\overline{\Sigma}_n^{C^2} > 0} \| \overline{\mathbf{v}}_n^{C^H} \overline{\mathbf{g}}(\mathbf{r}) \|^2 \tag{8}$$

where, $\overline{\Sigma}_n^{C^2}$ is the *n*-th significant eigen value, $\overline{\mathbf{v}}_n^C$ is the *n*-th eigen vector, and $\overline{\mathbf{g}}(\mathbf{r})$ is the background medium dyadic Green's function vector.

IV. Results

We consider a highly dense (class 4), low contrast breast phantom and embed two 10 mm sized tumors. The tumors are located around 2 o'clock and 4 o'clock position and 4.5 cm below the nipple. We obtain both conventional DORT and C-DORT images for the breast phantom as shown in Figs. 2-3 respectively for comparison. It can be observed from conventional DORT image in Fig. 2 that estimation of unambiguous tumor location is quite difficult. Further it is also difficult to predict the numbers of tumors present in the breast. There are significant side lobes and the image resolution is quite poor. A bright focus spot covers both the tumors as can be seen in the coronal view in Fig. 2(b). However, one can observe much improved result obtained from proposed C-DORT image as shown in Fig. 3. In this case, the tumor located at 2 o'clock position is estimated quite accurately with reduced side lobe levels. The tumor at 4 o'clock position shows weaker intensity but it is identifiable as a suspicious region. The improvement in the result due to coherent processing can be clearly demonstrable when compared with traditional DORT image in Fig. 2.

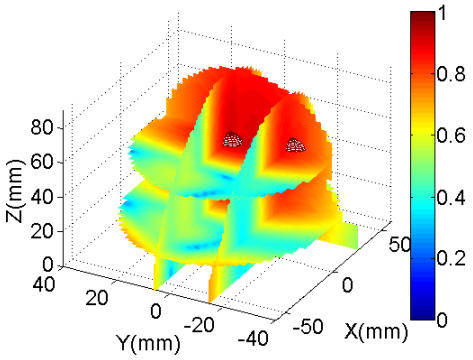

(a) 3D view

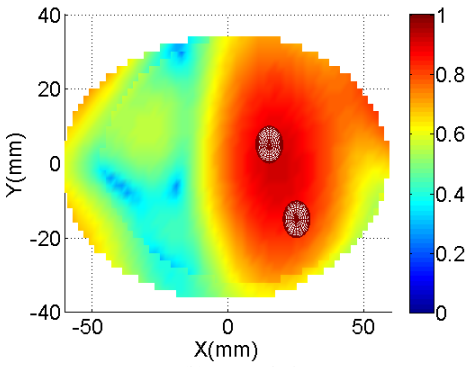

(b) coronal view

Fig 2. DORT imaging for the detection of two 10mm sized tumors.

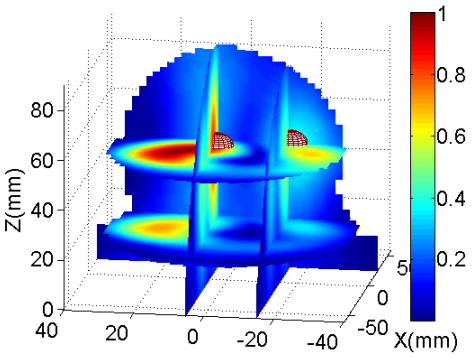

(a) 3D view

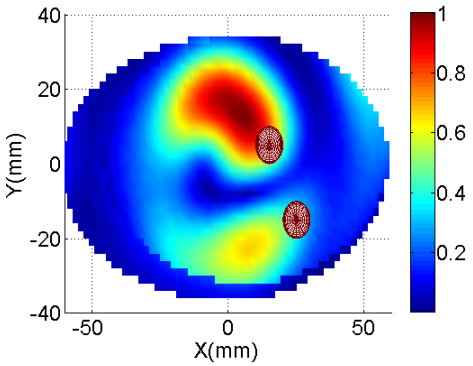

(b) coronal view

Fig 3. C-DORT imaging for the detection of two 10mm sized tumors.

V. CONCLUSION

Coherent processing helps to increase accuracy and resolution of conventional DORT imaging technique as can be seen by comparing the DORT and C-DORT imaging results for dense breast phantom. Although the scattered field is computed considering ideal antenna elements, realistic antennas can be used in actual experimental set-up without compromising imaging performance since the imaging bandwidth and microwave radiation requirements can be readily accommodated using existing antenna designs [16]. Tumor detection is a challenging issue in dense breasts and coherent processing has the potential to overcome the challenges. However, when closely spaced multiple tumors need to be localized, even C-DORT face limitations which arise mainly due to inherent limitations of the DORT technique.

REFERENCES

[1] A. J. Devaney, "Time reversal imaging of obscured targets from multistatic data," *IEEE Trans. Antennas Propag.,* vol. 53, pp. 1600-1610, 2005.

[2] D. H. Chambers and J. G. Berryman, "Analysis of the time-reversal operator for a small spherical scatterer in an electromagnetic field," *IEEE Trans. Antennas Propag.,* vol. 52, pp. 1729-1738, 2004.

[3] M. D. Hossain, A. S. Mohan, and M. J. Abedin, "Beamspace Time-Reversal Microwave Imaging for Breast Cancer Detection," *IEEE Antennas Wireless Propag. Lett.,* vol. 12, pp. 241-244, 2013.

[4] Y. Chen, E. Gunawan, L. Kay Soon, W. Shih-chang, K. Yongmin, and S. Cheong-Boon, "Pulse Design for Time Reversal Method as Applied to Ultrawideband Microwave Breast Cancer Detection: A Two-Dimensional Analysis," *IEEE Trans. Antennas Propag.,* vol. 55, pp. 194-204, 2007.

[5] Y. Chen, E. Gunawan, K. S. Low, S. c. Wang, C. B. Soh, and T. C. Putti, "Time-reversal ultrawideband breast Imaging: pulse design criteria considering multiple tumors with unknown tissue properties," *IEEE Trans. Antennas Propag.,* vol. 56, pp. 3073-3077, 2008.

[6] P. Kosmas and C. M. Rappaport, "FDTD-based time reversal for microwave breast cancer Detection-localization in three dimensions," *IEEE Trans. Microw. Theory Tech.,* vol. 54, pp. 1921-1927, 2006.

[7] P. Kosmas and C. M. Rappaport, "A matched-filter FDTD-based time reversal approach for microwave breast cancer detection," *IEEE Trans. Antennas Propag.,* vol. 54, pp. 1257-1264, 2006.

[8] M. D. Hossain and A. S. Mohan, "Coherent time-reversal microwave imaging for the detection and localization of breast tissue malignancies," *Radio Science,* vol. 50, pp. 87-98, 2015.

[9] M. Lazebnik, M. Okoniewski, J. H. Booske, and S. C. Hagness, "Highly accurate debye models for normal and malignant breast tissue dielectric properties at microwave frequencies," *IEEE Microw. Wireless Comp. Lett.,* vol. 17, pp. 822-824, 2007.

[10] M. Lazebnik, D. Popovic, L. McCartney, C. B. Watkins, M. a. J. Lindstrom, J. Harter, S. Sewall, T. Ogilvie, A. Magliocco, T. M. Breslin, W. Temple, D. a. Mew, J. H. Booske, M. i. Okoniewski, and S. C. H. agness, "A large-scale study of the ultrawideband microwave dielectric properties of normal, benign and malignant breast tissues obtained from cancer surgeries " *Phys. Med. Biol.,* vol. 52, pp. 6093–6115, 2007.

[11] A. M. Hassan and M. El-Shenawee, "Review of Electromagnetic Techniques for Breast Cancer Detection," *IEEE Rev. Biomed. Eng.,* vol. 4, pp. 103-118, 2011.

[12] H. Hung and M. Kaveh, "Focussing matrices for coherent signal-subspace processing," *IEEE Trans. Acoust. Speech Sig. Process.,* vol. 36, pp. 1272-1281, 1988.

[13] Y. Bucris, I. Cohen, and M. A. Doron, "Bayesian Focusing for Coherent Wideband Beamforming," *IEEE Trans. Audio, Speech, Language Process.,* vol. 20, pp. 1282-1296, 2012.

[14] *UWCEM breast phantom repository*. Available: https://uwcem.ece.wisc.edu/phantomRepository.html

[15] Z. Wanjun and F. Chin, "Entropy-based time window for artifact removal in UWB imaging of breast cancer detection," *IEEE Signal Process. Lett.,* vol. 13, pp. 585-588, 2006.

[16] A. M. Hassan and M. El-Shenawee, "Review of Electromagnetic Techniques for Breast Cancer Detection," *IEEE Reviews Biomed. Eng.,* vol. 4, pp. 103-118, 2011.